Nuclear Inst. and Methods in Physics Research B xxx (xxxx) xxx–xxx

Contents lists available at ScienceDirect

Nuclear Inst. and Methods in Physics Research B

journal homepage: www.elsevier.com/locate/nimb

The performance of the cryogenic buffer-gas stopping cell of SHIPTRAP

O. Kaleja[a,b,c,*], B. Anđelić[d,e], K. Blaum[a], M. Block[b,c,e], P. Chhetri[c,f], C. Droese[g], Ch.E. Düllmann[b,c,e], M. Eibach[c,g], S. Eliseev[a], J. Even[d], S. Götz[b,c,e], F. Giacoppo[c,e], N. Kalantar-Nayestanaki[d], M. Laatiaoui[b,c,e], E. Minaya Ramirez[h], A. Mistry[c,e], T. Murböck[c], S. Raeder[c], L. Schweikhard[g], P.G. Thirolf[i]

[a] Max-Planck-Institut für Kernphysik, Saupfercheckweg 1, 69117 Heidelberg, Germany
[b] Johannes Gutenberg-Universität Mainz, Saarstraße 21, 55122 Mainz, Germany
[c] GSI Helmholtzzentrum für Schwerionenforschung, Planckstraße 1, 64291 Darmstadt, Germany
[d] KVI-CART, University of Groningen, Zernikelaan 25, 9747 AA Groningen, Netherlands
[e] Helmholtz Institut Mainz, Johann-Joachim-Becherweg 36, 55128 Mainz, Germany
[f] Technische Universität Darmstadt, Schloßgartenstraße 7, 64289 Darmstadt, Germany
[g] Institut für Physik, Universität Greifswald, Felix-Hausdorff-Str. 6, 17489 Greifswald, Germany
[h] Institut de Physique Nucléaire d'Orsay-IN2P3-CNRS, Université Paris-Sud, 15 rue Georges Clemenceau, 91406 Orsay, France
[i] Ludwig-Maximilians-Universität München, Am Coulombwall 1, 85747 Garching, Germany

ARTICLE INFO

Keywords:
Cryogenic gas stopping cell
Stopping and extraction efficiency
Extraction time
Penning traps
Mass spectrometry
Fusion-evaporation reaction products
Transfermium elements
nobelium

ABSTRACT

Direct high-precision mass spectrometry of the heaviest elements with SHIPTRAP, at GSI in Darmstadt, Germany, requires high efficiency to deal with the low production rates of such exotic nuclides. A second-generation gas stopping cell, operating at cryogenic temperatures, was developed and recently integrated into the relocated system to boost the overall efficiency. Offline measurements using ^{223}Ra and ^{225}Ac recoil-ion sources placed inside the gas volume were performed to characterize the gas stopping cell with respect to purity and extraction efficiency. In addition, a first online test using the fusion-evaporation residue ^{254}No was performed, resulting in a combined stopping and extraction efficiency of 33(5)%. An extraction time of 55(44) ms was achieved. The overall efficiency of SHIPTRAP for fusion-evaporation reaction products was increased by an order of magnitude to 6(1)%. This will pave the way for direct mass spectrometry of heavier and more exotic nuclei, eventually in the region of superheavy elements with proton numbers $Z \geqslant 104$.

1. Introduction

SHIPTRAP [1] is a double Penning-trap mass spectrometer located behind the separator for heavy ion reaction products (SHIP) [2] at the end of the universal linear accelerator (UNILAC) [3] at the GSI Darmstadt, Germany. It is suitable for direct high-precision mass measurements of the heaviest elements, produced in fusion-evaporation reactions. Far away from stability, these species exhibit unique atomic and nuclear properties [4,5]. In this region the production cross sections rapidly drop from microbarn in the case of ^{254}No (proton number $Z = 102$) down to the order of picobarn for heavier elements around $Z = 114$. This results in production rates of a few ions per second down to single ions per week for typical beam intensities. Direct high-precision Penning-trap mass spectrometry (PTMS) requires stopping, thermalization and preparation of the ion of interest. Gas cells fulfill these tasks, however, with limited efficiency. In pioneering experiments, PTMS was extended to heavy nuclei with production rates down to only a few ions per minute at the SHIPTRAP experiment [6–8]. In these experiments the masses of $^{252\text{-}255}$No ($Z = 102$) and ^{255,256}Lr ($Z = 103$) were measured directly for the first time using the Time-of-Flight Ion-Cyclotron-Resonance (ToF-ICR) technique with relative uncertainties in the range of $\delta m/m = 10^{-7}$ to $\delta m/m = 10^{-8}$[6,7]. The low production rates and overall efficiency of the setup resulted in a challenging measurement time of 93 h in the case of ^{256}Lr for a resonance with just 48 detected ions [8]. Longer measurement times are prohibited by time-dependent drifts of the magnetic field. Therefore, to extend high-precision PTMS to more exotic or heavier nuclei, the decrease in production rate has to be compensated by an increase in efficiency and sensitivity of the setup.

With the recent development of the phase-sensitive Phase-Imaging

This article comprises results of the doctoral thesis of O. Kaleja.

* Corresponding author at: GSI Helmholtzzentrum für Schwerionenforschung, Planckstraße 1, 64291 Darmstadt, Germany.
E-mail address: o.kaleja@gsi.de (O. Kaleja).

https://doi.org/10.1016/j.nimb.2019.05.009
Received 14 January 2019; Received in revised form 23 April 2019; Accepted 3 May 2019
0168-583X/ © 2019 Elsevier B.V. All rights reserved.

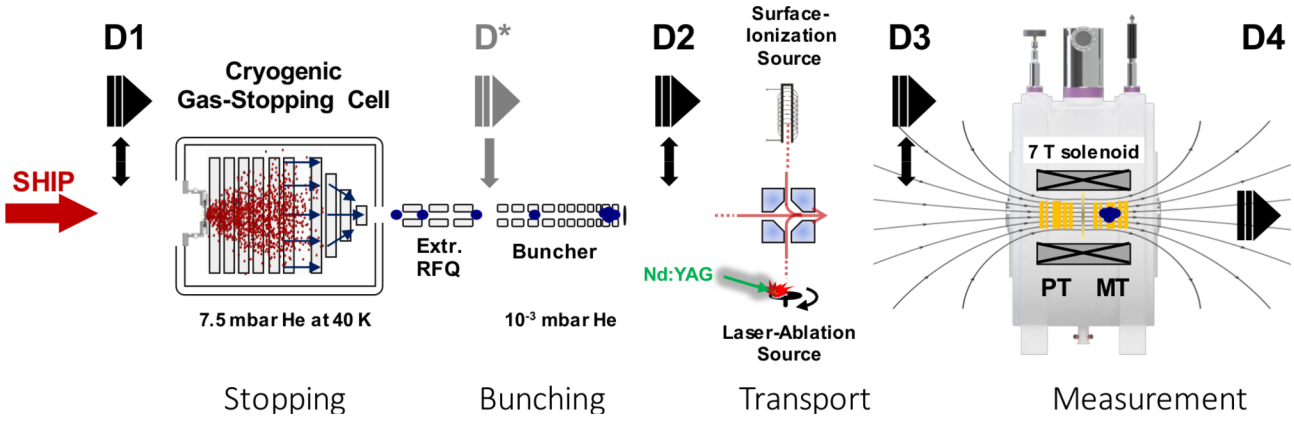

Fig. 1. Schematic view of the SHIPTRAP setup after relocation and implementation of the cryogenic gas stopping cell to stop the evaporation residues after their in-flight separation at SHIP. Further steps include ion guiding, bunching, transport, preparation and finally the high-precision PTMS. D1 to D4 indicate detector positions. The detector position D* was temporarily used. For further explanations see text.

Ion-Cyclotron-Resonance (PI-ICR) technique [9,10], the mass resolving power of direct mass measurements was improved by a factor of 40. Furthermore, this technique requires less ion counts than the ToF-ICR technique.

In addition, the overall efficiency is increased utilizing the cryogenic gas stopping cell [11]. It was implemented at the SHIPTRAP experiment, requiring the rearrangement of the whole beamline from a perpendicular [1] to a close-to-zero-degree position with respect to SHIP [12]. An overview of the current setup is given in Fig. 1 and will be briefly explained in the following.

2. Experimental setup

The production of transuranium elements requires complete fusion reactions using high-intensity heavy-ion beams at Coulomb barrier energies of about 5 MeV/u. The primary beam with a typical intensity of about 1 particle μA hits a rotating target wheel. The fusion-evaporation reaction products have characteristic recoil energies in the order of tens of MeV, i.e. about seven orders of magnitude higher than the energy acceptance of Penning traps.

After their in-flight separation from the primary beam by the velocity filter SHIP, the recoil ions pass optional degrader foils and an entrance-window foil before being stopped inside the gas volume of the cryogenic gas cell (He gas density typically 50 mbar room temperature equivalent). Following their thermalization, the ions are guided by electric fields towards an extraction nozzle of *de Laval*-type, where a gas-jet is formed. During their extraction the ions collide with residual buffer gas atoms. In the absence of any gas impurities the charge-state of the ions is only determined by the ionization potentials of the ion and the buffer gas atoms, thus usually singly or doubly charged. Due to unavoidable gas impurities on the parts-per-billion scale, the charge states are shifted towards lower-charged states and some of the ions neutralize inside the gas volume and are lost for extraction. It is of interest to measure ions in high charge states as the mass resolving power and precision of PTMS scales with the inverse of the mass-to-charge ratio of the ions.

After their extraction from the cell, the ions enter two consecutive radio-frequency quadrupole (RFQ) ion guide sections. In the first section (extraction RFQ), the carrier gas is pumped away, while the ions are guided into the second section (buncher). Here, the ions are cooled and bunched using ultra-pure He buffer-gas at a pressure of about 10^{-3} mbar. Further ion optical elements ensure an efficient ion transport and injection into the double Penning-trap system located inside the bore of a 7 T superconducting solenoid.

The first trap - preparation trap (PT) – is used for ion preparation and provides mass-selective buffer-gas cooling [13]. Its mass resolving power is in the order of 100,000 and allows isobaric separation. In the second trap - measurement trap (MT) – the cyclotron frequency $\nu_c = (2\pi)^{-1}(q/m)B$ of the ions is measured with either the PI-ICR or the ToF-ICR technique. At the exit of the magnet bore, ions are guided through a drift section towards a detector system comprising an MCP detector coupled with a resistive delay line allowing position-sensitive ion detection.

To determine the magnetic field strengths with sufficient precision, the cyclotron frequency of well-known reference ions is measured. To minimize systematic effects, the mass-to-charge ratio difference between reference ion and ion of interest is kept small, preferably by using isobars as reference [14]. In the case of transfermium elements various ion species from a laser-ablation or surface-ion source are used, including carbon cluster ions [14,15].

3. The cryogenic gas stopping cell

The first-generation gas stopping cell used in previous experiments for the direct mass measurements of No and Lr isotopes [6,7] had a combined stopping- and extraction efficiency of 4–8% [16–18] limiting the overall efficiency of the setup. Therefore, a second-generation gas stopping cell was developed, which operates at cryogenic temperatures and features a larger stopping volume. A detailed description of the cryogenic gas stopping cell (further referred to as cell) can be found in [11]. For the upcoming discussions a brief overview is given in the following:

The cell consists of a chamber filled with ultra-pure He gas at pressures around 50 mbar (room temperature-equivalent) where the ions are stopped and thermalized. This chamber can be cooled down to 40 K using a cryo cooler (type SUMITOMO SRDK-400) and is therefore located inside an evacuated chamber containing multi-layer insulation foils for thermal insulation. The gas-filled volume is separated from the high-vacuum regime of the velocity filter SHIP by a 3–4 μm thick titanium entrance-window foil through which ions enter into the cell. After their thermalization, the ions are guided towards an extraction nozzle of *de Laval*-type [19] by electric DC field gradients created by ring electrodes. In front of the extraction nozzle the ring electrodes are reduced in diameter and an additional electric RF field is applied to repel the ions and guide them towards the center (funnel structure [20]). At the end of the funnel, the ion guidance is achieved by the gas-flow in a supersonic jet into the low-pressure regime [19].

Compared to the first-generation gas stopping cell, the operation at cryogenic temperatures ensures the freeze-out of gas-impurities, decreasing the ion losses due to neutralization, improving the extraction efficiency by a factor of five [11,21,22]. In addition, the cryogenic environment shifts the charge-state distribution towards higher charged

states and reduces the abundance of molecular compounds.

4. Measurements

Fig. 1 indicates five different detector positions D* and D1 to D4 along the setup, which will be briefly discussed. Except D* and D4, all detectors are mounted on feedthroughs and can be moved in and out the beamline. D* was used temporarily to measure the performance of the cell in the case of fusion-evaporation reaction products from SHIP. D1 comprises a 16-strip silicon detector (type CANBERRA PF-16RT-1CT-3580-300) [23] which allows the measurement of the rate of incoming ions as well as the spatial distribution of the incoming ion beam. D*, D2 and D3 comprise an α-detector (type ORTEC TU-016-150-100) with a resolution of 120 keV (FWHM), sufficient to resolve the relevant α-lines from the decay of the extracted ions. The α-detectors are used to determine the extracted ion rate at their corresponding location for efficiency measurements. To this end, the ions are implanted in a 0.8 µm thick aluminium foil biased with −1.7 kV and placed at a distance of 9 mm in front of the detector. This detector-foil assembly is identical to the one used in [11]. In addition, D2 and D3 contain a Channeltron (type SJUTS KBL25RS) and MCP plates in chevron configuration (type TOPAG MCP-MA25/2), respectively, which are used to measure the time-of-flight distribution of the ions extracted from the buncher. The mass resolving powers are on the order of 100 (D2) and 200 (D3), sufficient to resolve the time-of-flight peaks of the ions emitted by the recoil-ion sources.

Time-of-flight measurements also give access to charge-state distributions and can reveal the presence of molecular compounds. They are therefore used to monitor the purity of the system. In addition, important parameters, e.g., the voltage difference between the extraction nozzle and the last funnel electrode, can be optimized for different charge-states and ion species. Following the Penning traps, a position-sensitive MCP detector (type ROENTDEK DLD40) [9] is installed at D4 to measure the transversal position and the time of flight of the ions required to perform mass measurements with the PI-ICR or ToF-ICR technique, respectively. This is also used to identify the ions observed by their time of flights measured at D2 or D3.

5. Offline studies

In order to characterize the performance of the system, ^{223}Ra ($T_{1/2}$ = 11.43(5) d) and ^{225}Ac ($T_{1/2}$ = 10.0(1) d) recoil-ion sources were placed inside the gas volume of the cell at different positions. In previous measurements the extraction efficiency of the cell was determined to be 74(3)% at cryogenic temperatures using an α-detector-foil assembly placed behind the extraction RFQ at D*[11].

5.1. Extraction time vs. extraction efficiency

The extraction efficiency of the cell is sensitive to the voltage difference between the extraction nozzle V_{noz} and the last electrode of the funnel V_{Fun}^{min}. Fig. 2 shows the signal of the extracted ions as a function of the voltage difference. Compared to [11] the maximum shifted from −4.6 V to about 0 V at 45 K for an axial source position of about 20 cm in front of the extraction nozzle. This is attributed to an axial misalignment between the extraction nozzle and the funnel during the old measurements that has been corrected meanwhile. Using the same technique as described in [11] (pulsed source voltage combined with a delay-pulsed extraction RFQ), additional measurements on the extraction time were performed. Fig. 2(b) shows the ion signal as a function of the extraction time for different nozzle-to-funnel voltage differences and DC gradients. It can be seen that there is a trade-off between the fastest extraction and highest extraction efficiency. Currently, the nuclides of interest for high-precision PTMS at SHIPTRAP are relatively long-lived, typically exceeding half-lives of one second. Therefore, the cell operates at maximum efficiency.

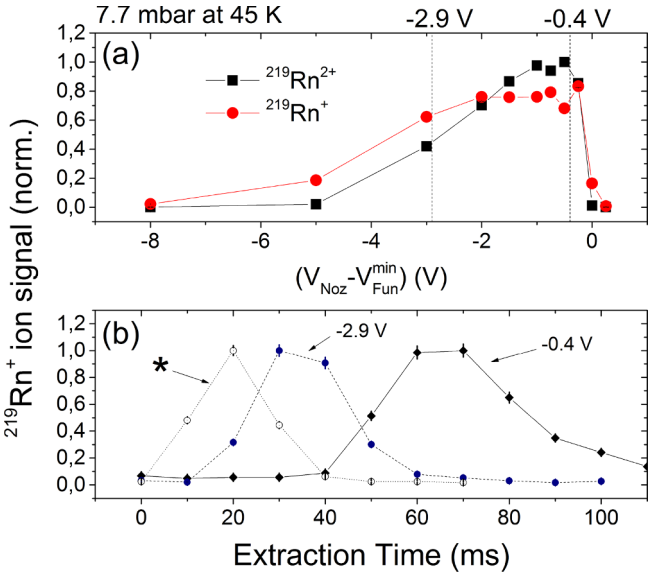

Fig. 2. Signal of the extracted ions from a ^{223}Ra recoil-ion source as a function of the voltage difference between the extraction nozzle and closest funnel electrode (a) and the extraction time (b) at a gas pressure of 7.7 mbar with an operating temperature of 45 K measured at D3. The source was placed 20 cm in front of the funnel with a DC gradient of 1.6 V/cm. The extraction time curves were measured at a voltage difference between the extraction nozzle and closest funnel electrode of −0.4 V and −2.9 V, respectively. * corresponds to −2.9 V with a higher funnel DC gradient of 3.5 V/cm along the funnel. To obtain the extraction time in (b) a pulsed source voltage in combination with a delay-pulsed extraction RFQ was used.

5.2. Charge-state distribution and purity

By integrating the cell into the SHIPTRAP setup, it is now possible to analyze its purity by measuring charge-state distributions. The charge-state distribution for the extracted isotopes is element specific and depends on the ionization potentials of the corresponding isotope of interest relative to those of the He buffer gas. If present in the gas in sufficient amounts, any impurity, in particular those with low ionization potentials, will shift the charge-state distribution towards lower charged states and reduce the extraction efficiency due to neutralization. Fig. 3 shows a time-of-flight spectrum (ejection pulse from the buncher) at D3 originating from the ^{223}Ra recoil-ion source located inside the cell. Bi and Pb are primarily extracted as doubly charged ions. The charge-state distribution of Rn is in the order of 60% doubly charged and 40% singly charged ions. This can be explained by the low second ionization potential of Bi and Pb of 16.7 eV [24,25] and 15.0 eV

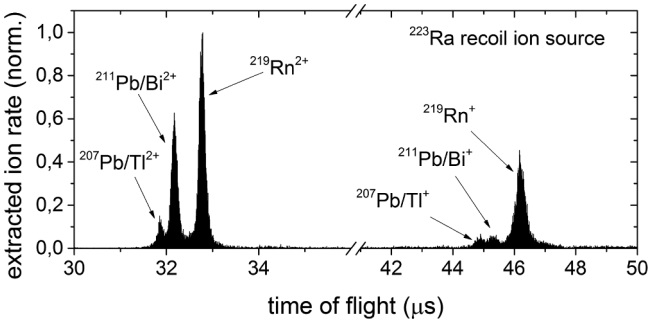

Fig. 3. Time-of-flight spectrum of extracted ions from a ^{223}Ra recoil-ion source located inside the cell (placed 20 cm in front of the extraction nozzle) measured at D3. The gas pressure was 7.3 mbar at an operating temperature of 40 K. The buncher was operated at 100 V_{pp} with a buncher accumulation time of 40 ms. The starting time corresponds to the ejection pulse from the buncher.

[26], respectively, compared to the second ionization potential of Rn of 21.4 eV [27]. By increasing the distance between the recoil-ion source and the extraction nozzle inside the gas volume from ≈20 cm to ≈45 cm, doubly charged Rn vanishes, while the charge-state distribution of Pb is less affected than that of Bi. This indicates that in the present state the cell's purity is limited by the presence of atomic or molecular impurities with ionization potentials in the range of 15 eV to 16 eV. Possible candidates are Ar (15.8 eV [28]), N_2 (15.6 eV [29]) and H_2 (15.4 eV [30]). However, only the latter may be expected to be present at an operating temperature of 40 K.

6. Online performance

To compare its performance with the first-generation gas stopping cell on fusion-evaporation reaction products, the cell was tested online during the beam time period at GSI in 2015 using ^{254}No ions produced in the reaction ^{208}Pb(^{48}Ca, 2n). The cross section of 2 µb [31] resulted in an incoming ion rate of about 3 ions/s for a beam intensity of 0.6 particle µA, measured at D1 about 150 cm in front of the cell. After their thermalization and extraction from the cell the ions were guided via the extraction RFQ onto a thin aluminium foil where their identification by characteristic α-emission took place. For this the buncher had been removed and the detector D* installed (see also Fig. 1).

6.1. Stopping- and extraction efficiency

The cell has an overall efficiency

$$\epsilon_{\text{cell}} = \epsilon_{\text{geom}}\,\epsilon_{\text{stop}}\,\epsilon_{\text{extr}} \tag{1}$$

where the geometric efficiency $\epsilon_{\text{geom}} = 89(3)\%$ considers the finite entrance-window size in comparison with the beam profile (4(1)% losses) and the grid structure supporting the entrance-window foil (7(3)% losses). The beam profile was measured at D1 [23]. ϵ_{stop} and ϵ_{extr} are the stopping- and extraction efficiency, respectively. With this setup the cell efficiency ϵ_{cell} was determined according to

$$\epsilon_{\text{cell}} = \frac{\dot{n}_{\text{D}^*}}{\dot{n}_{\text{D1}}} \text{ with } \dot{n}_{\text{D}^*} = \frac{\dot{\alpha}}{\mu\,\epsilon^{\text{det}}} \tag{2}$$

where $\dot{n}_{\text{D1}}$ is the incoming ion rate measured at D1 and $\dot{n}_{\text{D}^*}$ is the extracted ion rate at D*. The latter can be deduced from the activity measurement $\dot{\alpha}$ where $\epsilon^{\text{det}} = 16(1)\%$ is the geometrical detector efficiency [11] and $\mu = 90(4)\%$ is the α-branching ratio of the detected α-decay of ^{254}No [32]. The detection efficiency for α-particles is assumed to be 100% [11].

Fig. 4(a) shows a measured α-decay spectrum of the extracted ^{254}No ions. The highest efficiency of $\epsilon_{\text{cell}} = 33(5)\%$ was found at the lowest temperature probed, namely 90 K [22] (see Fig. 4(b)). Due to the limited time available during the online beam time the cell could not be cooled to the nominal operation temperature of 40 K. The gas pressure was 20 mbar at 90 K and a titanium entrance-window foil with a thickness of 3.8 µm was used. Taking into account the measured offline extraction efficiency of $\epsilon_{\text{extr}} = 74(3)\%$ [11], a stopping efficiency of $\epsilon_{\text{stop}} = 50(8)\%$ was deduced. This is in agreement with simulations based on the SRIM code [33], indicating that a fraction of about 40% of the ions is already stopped within the entrance-window foil and, thus, lost. For lower gas temperatures and an optimized entrance-window thickness and gas density, further improvements in efficiency are expected. Thinner entrance-window foils in combination with a higher He gas pressure are favorable. An increase in the pressure has to be compensated by an increased repulsive force from the funnel on the ions. The RF amplitude of the funnel is currently limited to about 150 V (peak-to-peak), limiting the maximum He gas pressure to about 60 mbar at room remperature. An optimized entrance-window foil thickness of about 3.3 µm at 60 mbar room temperature equivalent will increase the stopping efficiency to about 80(10)% for ^{254}No ions. Because of the relatively low second ionization potential of No of 12.9 eV [24] compared to Pb (see Section 5.2), it is expected that No was predominantly extracted as doubly charged ion.

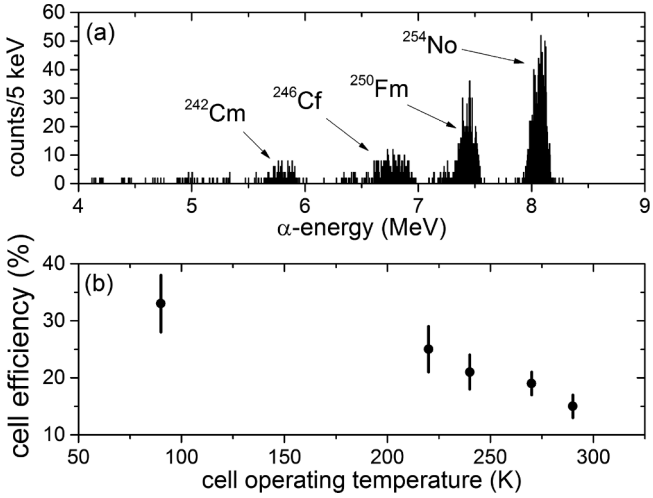

Fig. 4. (a) α-decay spectrum of extracted ^{254}No ions measured at D*. The data was summed over 21 successive measurements with a total measurement time of about 6600 s. (b) Cell efficiency ϵ_{cell} as a function of the cell operating temperature.

6.2. Stopping and extraction time

It is possible to estimate the time for stopping, thermalization and extraction of the fusion-evaporation products from the cell when measuring the extraction efficiencies of two isotopes with different half-lives. For this ^{154}Yb ($T_{1/2} = 409(2)$ ms) and ^{155}Yb ($T_{1/2} = 1793(19)$ ms) [34], produced in the reaction ^{112}Sn(^{48}Ca,xn) with a cross section of about 7 mb for ^{155}Yb [23,35], were investigated. Taking into account the decay constants of the isotopes under consideration, the rate of extracted ions is

$$\dot{n}_{\text{D}^*} = \dot{n}_{\text{D1}}\,\epsilon_{\text{cell}}\,\mathrm{e}^{-\lambda t_{\text{cell}}} \text{ with } t_{\text{cell}} = \frac{\ln(R_{\text{extr}}/R_{\text{inc}})}{\lambda_{\text{Yb155}} - \lambda_{\text{Yb154}}}, \tag{3}$$

where t_{cell} and λ are the combined stopping- and extraction time and decay constant of the ion, respectively. ϵ_{cell} is the cell efficiency given by Eq. (1). By comparing the peak intensity ratios of ^{154}Yb in relation to ^{155}Yb in front of the cell ($R_{\text{inc}} = 7.40(16)$ %) and after extraction ($R_{\text{extr}} = 6.91(37)$ %) one is able to deduce the combined stopping- and extraction time t_{cell}. This holds because the cell efficiency and α-detection efficiency are assumed to be the same for both isotopes (α-decay energy approximately the same for both isotopes). For the case of Yb with DC-field gradients of 7 V/cm and 3 V/cm applied to the DC cage and funnel, respectively, the combined stopping- and extraction time was $t_{\text{cell}} = 55(44)$ms for a gas pressure of 50 mbar at room temperature. The majority of the uncertainty originates from the low statistics of the extracted ^{154}Yb peak.

7. Overall efficiency of SHIPTRAP

Using a recoil-ion source inside the He gas volume of the cell one is able to measure the overall offline efficiency

$$\epsilon_{\text{offline}} \equiv \frac{\dot{n}_{\text{D4}}}{\dot{n}_{\text{recoil}}} = \epsilon_{\text{extr}}\,\epsilon_{\text{bun}}\,\epsilon_{\text{opt}}\,\epsilon_{\text{trap}}\,\epsilon_{\text{det}} \tag{4}$$

of the SHIPTRAP setup, i.e. the ratio between the detected ion signal rate $\dot{n}_{\text{D4}}$ at D4 and the rate of emitted recoil ions $\dot{n}_{\text{recoil}}$. Here, ϵ_{extr} is the extraction efficiency introduced in Eq. (1) where the assumption is made that the extraction efficiency for the point-like recoil-ion source is the same as for stopped fusion-evaporation reactions that was measured in Eq. (1). This ansatz is fulfilled in good approximation since the

Table 1
Offline efficiency of SHIPTRAP for the recoil ions ^{219}Rn and ^{221}Fr. The cell was operated at 7.6 mbar at 40 K and a full measurement cycle consisting of 200 ms cooling (preparation trap) and 200 ms accumulation time (measurement trap without any excitation) was used. (a) $\bar{\epsilon}_{\mathrm{offline}}$ corresponds to the uncertainty-weighted arithmetic mean value. (b) Cell efficiency from Section 6 and (c) online efficiency from Section 7. For further details see text.

	$\dot{n}_{\mathrm{recoil}}$	$\dot{n}_{\mathrm{D4}}$	$\epsilon_{\mathrm{offline}}$	$\bar{\epsilon}_{\mathrm{offline}}$	ϵ_{cell}	$\epsilon_{\mathrm{online}}$
^{219}Rn	82(2) s^{-1}	7.0(2) s^{-1}	8.6(3)%	8.7(3)%[a]	33(5)%[b]	6(1)%[c]
^{221}Fr	17(2) s^{-1}	1.80(5) s^{-1}	10.4(11)%			

distribution of stopped ions is well confined with respect to the He gas volume, as validated by SRIM simulations. ϵ_{bun} and ϵ_{opt} are the transmission efficiencies through the buncher and the subsequent ion optics, respectively, whereas ϵ_{trap} takes into account the trap-related efficiencies (e.g. injection and storage efficiency). ϵ_{det} corresponds to the detection efficiency of D4.

The efficiency measurements were performed using both the ^{223}Ra and ^{225}Ac ion sources located inside the cell. At D2 the partial efficiency

$$\epsilon_{\mathrm{extr}}\,\epsilon_{\mathrm{bun}} \equiv \frac{\dot{n}_{\mathrm{D2}}}{\dot{n}_{\mathrm{recoil}}} = 45(5)\% \tag{5}$$

was obtained, where the ion rate $\dot{n}_{\mathrm{D2}}$ was determined in the same way as described for Eq. (2). Table 1 gives an overview of the recoil-ion rate $\dot{n}_{\mathrm{recoil}}$ and the detected ion rate signal $\dot{n}_{\mathrm{D4}}$ at D4 for both recoil-ion sources, resulting in offline efficiencies of 8.6(3)% and 10.4(11)% for ^{219}Rn and ^{221}Fr, respectively. The uncertainty-weighted arithmetic mean results in an offline efficiency of $\bar{\epsilon}_{\mathrm{offline}} = 8.7(3)\%$. Assuming a detection efficiency of $\epsilon_{\mathrm{det}} = 30\%$ [36], the combined transmission and trap-related efficiency can be estimated to about $\epsilon_{\mathrm{opt}}\,\epsilon_{\mathrm{trap}} = 70\%$.

Table 1 allows to estimate an overall online efficiency

$$\epsilon_{\mathrm{online}} \equiv \frac{\dot{n}_{\mathrm{D4}}}{\dot{n}_{\mathrm{D1}}} = \underbrace{\epsilon_{\mathrm{geom}}\,\epsilon_{\mathrm{stop}}\,\epsilon_{\mathrm{extr}}}_{=\epsilon_{\mathrm{cell}}}\,\epsilon_{\mathrm{bun}}\,\epsilon_{\mathrm{opt}}\,\epsilon_{\mathrm{trap}}\,\epsilon_{\mathrm{det}} = 6(1)\%, \tag{6}$$

of SHIPTRAP on fusion-evaporation reaction products, where an optimized stopping efficiency of $\epsilon_{\mathrm{stop}} = 80(10)\%$ was assumed (see Section 6.1). Compared to the overall efficiency of the old setup of 0.5% [1], this is a boost in efficiency of a factor of 12. This will pave the way for direct high-precision PTMS of heavier and more exotic nuclei, bringing the region of the superheavy elements with proton numbers of $Z \geqslant 104$ within reach.

8. Summary and outlook

A cryogenic gas stopping cell was recently implemented into the SHIPTRAP setup. Its performance was characterized by the evaluation of data obtained from offline and online measurements using time-of-flight and α-spectra. A trade-off between extraction efficiency and extraction time was established. The offline efficiency for the SHIPTRAP setup with recoil-ion sources placed inside the He gas volume of the cell was measured to be 8.7(3)%. For the cell efficiency on the fusion-evaporation reaction product ^{254}No a value of 33(5)% was obtained during the online commissioning. Combining this information, an overall online efficiency of the SHIPTRAP setup of 6(1)% is estimated in the case of an optimized entrance-window thickness of the cell of 3.3 µm for ^{254}No ions. A combined stopping- and extraction time of 55(44) ms was obtained at room temperature for the fusion-evaporation reactions ^{154,155}Yb. To further improve the cell's purity at cryogenic temperatures, a non-evaporable getter (NEG) pump will be installed in the gas volume. This will in particular reduce the partial pressure of H_2.

Acknowledgments

The authors thank D. Renisch (Institute of Nuclear Chemistry Mainz) and P. Dendooven (University of Groningen) for providing recoil-ion sources. In addition, the authors thank D. Racano, H.-G. Burkhard and J. Maurer (GSI) for their suppportive engineering work. This work has been supported by the German BMBF (Grant No. 05P12HGFN5, 05P15HGFNA and 05P15UMFNA).

References

[1] M. Block, D. Ackermann, K. Blaum, A. Chaudhuri, Z. Di, S. Eliseev, R. Ferrer, D. Habs, F. Herfurth, F.P. Heßberger, S. Hofmann, H.-J. Kluge, G. Maero, A. Martín, G. Marx, M. Mazzocco, M. Mukherjee, J.B. Neumayr, W.R. Plaß, W. Quint, S. Rahaman, C. Rauth, D. Rodríguez, C. Scheidenberger, L. Schweikhard, P.G. Thirolf, G. Vorobjev, C. Weber, Towards direct mass measurements of nobelium at SHIPTRAP. The, Eur. Phys. J. D 45 (1) (2007) 39–45.

[2] G. Münzenberg, W. Faust, S. Hofmann, P. Armbruster, K. Güttner, H. Ewald, The velocity filter SHIP, a separator of unslowed heavy ion fusion products, Nucl. Instrum. Methods 161 (1) (1979) 65–82.

[3] W. Barth, W. Bayer, L. Dahl, L. Groening, S. Richter, S. Yaramyshev, Upgrade program of the high current heavy ion UNILAC as an injector for FAIR, Nucl. Instrum. Methods Phys. Res., Sect. A 577 (1–2) (2007) 211–214.

[4] M. Block. Direct mass measurements of the heaviest elements with penning traps. Int. J. Mass Spectrometry, 349–350:94–101, 2013. 100 years of Mass Spectrometry.

[5] M. Block, Direct mass measurements of the heaviest elements with penning traps, Nucl. Phys. A 944 (2015) 471–491.

[6] M. Block, D. Ackermann, K. Blaum, C. Droese, M. Dworschak, S. Eliseev, T. Fleckenstein, E. Haettner, F. Herfurth, F.P. Heßberger, S. Hofmann, J. Ketelaer, J. Ketter, H.-J. Kluge, G. Marx, M. Mazzocco, Yu.N. Novikov, W.R. Plaß, A. Popeko, S. Rahaman, D. Rodríguez, C. Scheidenberger, L. Schweikhard, P.G. Thirolf, G.K. Vorobyev, C. Weber, Direct mass measurements above uranium bridge the gap to the island of stability, Nature 463 (7282) (2010) 785–788.

[7] E.M. Ramirez, D. Ackermann, K. Blaum, M. Block, C. Droese, C.E. Dullmann, M. Dworschak, M. Eibach, S. Eliseev, E. Haettner, F. Herfurth, F.P. Hessberger, S. Hofmann, J. Ketelaer, G. Marx, M. Mazzocco, D. Nesterenko, Y.N. Novikov, W.R. Plass, D. Rodriguez, C. Scheidenberger, L. Schweikhard, P.G. Thirolf, C. Weber, Direct mapping of nuclear shell effects in the heaviest elements, Science 337 (6099) (2012) 1207–1210.

[8] M. Dworschak, M. Block, D. Ackermann, G. Audi, K. Blaum, C. Droese, S. Eliseev, T. Fleckenstein, E. Haettner, F. Herfurth, F.P. Heßberger, S. Hofmann, J. Ketelaer, J. Ketter, H.-J. Kluge, G. Marx, M. Mazzocco, Yu.N. Novikov, W.R. Plaß, A. Popeko, S. Rahaman, D. Rodríguez, C. Scheidenberger, L. Schweikhard, P.G. Thirolf, G.K. Vorobyev, M. Wang, C. Weber, Penning trap mass measurements on nobelium isotopes, Phys. Rev. C 81 (6) (2010) jun.

[9] S. Eliseev, K. Blaum, M. Block, C. Droese, M. Goncharov, E. Minaya Ramirez, D.A. Nesterenko, Yu. N. Novikov, L. Schweikhard, Phase-imaging ion-cyclotron-resonance measurements for short-lived nuclides, Phys. Rev. Lett. 110 (8) (2013).

[10] S. Eliseev, K. Blaum, M. Block, A. Dörr, C. Droese, T. Eronen, M. Goncharov, M. Höcker, J. Ketter, E. Minaya Ramirez, D.A. Nesterenko, Yu.N. Novikov, L. Schweikhard, A phase-imaging technique for cyclotron-frequency measurements, Appl. Phys. B 114 (1–2) (2013) 107–128.

[11] C. Droese, S. Eliseev, K. Blaum, M. Block, F. Herfurth, M. Laatiaoui, F. Lautenschläger, E. Minaya Ramirez, L. Schweikhard, V.V. Simon, and P.G. Thirolf. The cryogenic gas stopping cell of SHIPTRAP. Nucl. Instrum. Methods Phys. Res. Section B, 338:126–138, Nov 2014.

[12] F. Giacoppo, K. Blaum, M. Block, P. Chhetri, Ch.E. Düllmann, C. Droese, S. Eliseev, P. Filianin, S. Götz, Y. Gusev, F. Herfurth, F.P. Hessberger, O. Kaleja, J. Khuyagbaatar, M. Laatiaoui, F. Lautenschläger, C. Lorenz, G. Marx, E. Minaya Ramirez, A. Mistry, Yu.N. Novikov, W.R. Plass, S. Raeder, D. Rodríguez, D. Rudolph, L.G. Sarmiento, C. Scheidenberger, L. Schweikhard, P. Thirolf, A. Yakushev, Recent upgrades of the SHIPTRAP setup: On the finish line towards direct mass spectroscopy of superheavy elements, Acta Phys. Pol., B 48 (3) (2017) 423.

[13] G. Savard, S.T. Becker, G. Bollen, H.-J. Kluge, R.B. Moore, Th. Otto, L. Schweikhard, H. Stolzenberg, U. Wiess, A new cooling technique for heavy ions in a penning trap, Phys. Lett. A 158 (5) (1991) 247–252.

[14] A. Chaudhuri, M. Block, S. Eliseev, R. Ferrer, F. Herfurth, A. Martín, G. Marx, M. Mukherjee, C. Rauth, L. Schweikhard, G. Vorobjev, Carbon-cluster mass calibration at SHIPTRAP, Eur. Phys. J. D 45 (1) (2007) 47–53.

[15] K. Blaum, G. Bollen, F. Herfurth, A. Kellerbauer, H.-J. Kluge, M. Kuckein, E. Sauvan, C. Scheidenberger, L. Schweikhard, Carbon clusters for absolute mass measurements at ISOLTRAP. The, Eur. Phys. J. A 15(1), 245–248 (2002) sep.

[16] J.B. Neumayr, L. Beck, D. Habs, S. Heinz, J. Szerypo, P.G. Thirolf, V. Varentsov, F. Voit, D. Ackermann, D. Beck, M. Block, Z. Di, S.A. Eliseev, H. Geissel, F. Herfurth, F.P. Heßberger, S. Hofmann, H.-J. Kluge, M. Mukherjee, G. Münzenberg, M. Petrick, W. Quint, S. Rahaman, C. Rauth, D. Rodríguez, C. Scheidenberger, G. Sikler, Z. Wang, C. Weber, W.R. Plaß, M. Breitenfeldt, A. Chaudhuri, G. Marx, L. Schweikhard, A.F. Dodonov, Y. Novikov, M. Suhonen, The ion-catcher device for SHIPTRAP, Nucl. Instrum. Methods Phys. Res., Sect. B 244 (2) (2006) 489–500.

[17] Guy Savard, Large radio-frequency gas catchers and the production of radioactive nuclear beams, J. Phys: Conf. Ser. 312 (5) (2011) 052004.

[18] S.A. Eliseev, M. Block, A. Chaudhuri, Z. Di, D. Habs, F. Herfurth, H.-J. Kluge, J.B. Neumayr, W.R. Plaß, C. Rauth, P.G. Thirolf, G. Vorobjev, Z. Wang, Extraction efficiency and extraction time of the SHIPTRAP gas-filled stopping cell, Nucl. Instrum. Methods Phys. Res., Sect. B 258 (2) (2007) 479–484.

ARTICLE IN PRESS

[19] T.-C. Jen, L. Pan, L. Li, Q. Chen, W. Cui, The acceleration of charged nano-particles in gas stream of supersonic de-laval-type nozzle coupled with static electric field, Appl. Therm. Eng. 26 (5–6) (2006) 613–621.

[20] M. Wada, Y. Ishida, T. Nakamura, Y. Yamazaki, T. Kambara, H. Ohyama, Y. Kanai, T.M. Kojima, Y. Nakai, N. Ohshima, A. Yoshida, T. Kubo, Y. Matsuo, Y. Fukuyama, K. Okada, T. Sonoda, S. Ohtani, K. Noda, H. Kawakami, I. Katayama, Slow RI-beams from projectile fragment separators, Nucl. Instrum. Methods Phys. Res., Sect. B 204 (2003) 570–581.

[21] S. Eliseev, M. Block, M. Dworschak, F. Herfurth, H.-J. Kluge, A. Martin, C. Rauth, G. Vorobjev, A new cryogenic gas-filled stopping chamber for SHIPTRAP, Nucl. Instrum. Methods Phys. Res., Sect. B 266 (19–20) (2008) 4475–4477.

[22] O. Kaleja, K. Blaum, M. Block, P. Chhetri, S. Eliseev, F. Giacoppo, F.-P. Heßberger, M. Laatiaoui, F. Lautenschläger, E. Minaya-Ramirez, A. Mistry, S. Raeder, L. Schweikhard, P. Thirolf, GSI Sci. Rep. (2015) 2016, https://doi.org/10.15120/gr-2016-1.

[23] F. Lautenschläger, P. Chhetri, D. Ackermann, H. Backe, M. Block, B. Cheal, A. Clark, C. Droese, R. Ferrer, F. Giacoppo, S. Götz, F.P. Heßberger, O. Kaleja, J. Khuyagbaatar, P. Kunz, A.K. Mistry, M. Laatiaoui, W. Lauth, S. Raeder, Th. Walther, C. Wraith, Developments for resonance ionization laser spectroscopy of the heaviest elements at SHIP, Nucl. Instrum. Methods Phys. Res., Sect. B 383 (2016) 115–122 sep.

[24] A. Kramida, Yu. Ralchenko, J. Reader, and NIST ASD Team. Nist atomic spectra database (version 5.6.1). Online, 2018. Available at https://physics.nist.gov/asd, accessed 14.12.2018.

[25] Y.N. Joshi, M. Mazzoni, The $6s_26p_23P_0$-$6s_26p$ nd $^3D_1$ series in photoabsorption of Bi II, Phys. Lett. A 118 (5) (1986) 237–238.

[26] M.E. Hanni, Julie A. Keele, S.R. Lundeen, C.W. Fehrenbach, W.G. Sturrus, Polarizabilities of Pb^{2+} and Pb^{4+} and ionization energies of Pb^+ and Pb^{3+} from spectroscopy of high-L Rydberg states of Pb^+ and Pb^{3+}, Phys. Rev. A 81 (4) (2010).

[27] W. Finkelnburg, W. Humbach, Ionisierungsenergien von Atomen und Atomionen, Die Naturwissenschaften 42 (2) (1955) 35–37.

[28] I. Velchev, W. Hogervorst, W. Ubachs, Precision VUV spectroscopy of Ar I at 105 nm, J. Phys. B: At. Mol. Opt. Phys. 32 (17) (1999) L511–L516.

[29] T. Trickl, E.F. Cromwell, Y.T. Lee, A.H. Kung, State-selective ionization of nitrogen in the x2 = 0 and v = 1 states by two-color (1 + 1) photon excitation near threshold, J. Chem. Phys. 91 (10) (1989) 6006–6012.

[30] D. Shiner, J.M. Gilligan, B.M. Cook, W. Lichten, H_2, D_2, and HD ionization potentials by accurate calibration of several iodine lines, Phys. Rev. A 47 (5) (1993) 4042–4045.

[31] A.V. Belozerov, M.L. Chelnokov, V.I. Chepigin, T.P. Drobina, V.A. Gorshkov, A.P. Kabachenko, O.N. Malyshev, I.M. Merkin, Yu. Ts, A.G. Oganessian, R.N. Popeko, A.I. Sagaidak, A.V. Svirikhin, G. Yeremin, I. Brida Berek, Š. Šáro, Spontaneous-fission decay properties and production cross-sections for the neutron-deficient nobelium isotopes formed in the $^{44,48}Ca + {}^{204,206,208}Pb$ reactions, Eur. Phys. J. A 16 (4) (2003) 447–456.

[32] M. Wang, G. Audi, A.H. Wapstra, F.G. Kondev, M. MacCormick, X. Xu, B. Pfeiffer, The ame2012 atomic mass evaluation, Chinese Phys. C 36 (12) (2012) 1603.

[33] J.F. Ziegler, M.D. Ziegler, J.P. Biersack, SRIM – the stopping and range of ions in matter, Nucl. Instrum. Methods Phys. Res. Section B 268 (11–12) (2010) 1818–1823.

[34] S.K. Basu, A.A. Sonzogni, Nuclear Data Sheets for A = 150, Nucl. Data Sheets 114 (4–5) (2013) 435–660.

[35] W. Reisdorf, M. Schädel, How well do we understand the synthesis of heavy elements by heavy-ion induced fusion? Zeitschrift für Physik A Hadrons and Nuclei 343 (1) (1992) 47–57.

[36] G. Eitel, M. Block, A. Czasch, M. Dworschak, S. George, O. Jagutzki, J. Ketelaer, J. Ketter, Position-sensitive ion detection in precision penning trap mass spectrometry, Nucl. Instrum. Methods Phys. Res. Section A 606 (3) (2009) 475–483.